J. Environ. Nanotechnol.
Volume 8, No.1(2019) pp.52 - 67
ISSN (Print): 2279-0748
ISSN (Online): 2319-5541
doi:10.13074/jent.2019.03.191357

Nio @ Paraffin Wax Soot Carbon Nano Composites for Congo Red Dye Removal from Waste Water

I. Muralisankar[1*], S. Agilan[2], T. Venkatachalam[3], E. P. Subramaniam[4], P. Thanapackiam[5]

[*1,4,5]*Department of Chemistry, Coimbatore Institute of Technology, Coimbatore, TN, India.*
[2,3]*Department of Physics, Coimbatore Institute of Technology, Coimbatore, TN, India.*

Received: 08.11.2018 *Accepted: 22.12.2018*

Abstract

Nickel oxide activated carbon nanocomposites (NiO-CNC), synthesized using the carbon soot of paraffin wax by a simple combustion method and tested as an adsorbent for the removal of hazardous Congo red dye (CR) in aqueous phase is presented in this work. The adsorption studies have been investigated thoroughly and elucidated with the impact of important parameters, pH of the dye solution, initial dye concentration, contact time and sorbent dose, which were found to be 11, 200 ppm, 60 min., and 0.035 g/L, respectively. Sorption kinetics and isotherm modeling were studied and checked for their applicability with dye sorption system using synthesized NiO-CNC by non-linear fit. The Co-relation coefficient of Langmuir and Redlich-peterson isotherm model is found to be 0.99 > 1 which explains the adsorption mechanism. Pseudo-second order kinetic model fits well with the obtained equilibrium data with maximum sorption capacity (q_e= 401.35 mg/g). The thermodynamic parameters indicate that NiO-CNC system is more feasible, exothermic and spontaneous.

Keywords : *Carbon nanocomposite; Nickel oxide; Non-linear fit; Sorption kinetics; Thermodynamic studies.*

1. INTRODUCTION

Toxic effluents from textile, metal finishing, leather, plastics and paper industries contain various types of synthetic dyes, which pollute the water bodies. All these industries consume large amounts of water since there are different stages of processing, dyeing and for the completion of products. Synthetic dyes used in these industries are highly toxic and visible, and even small amount of dyes is sufficient to contaminate the entire water system. Hence removal of these dyes from such contaminated water before entering into the environment has become a major concern (Gong *et al.* 2009; Shahryari-Ghoshekandi and Sadegh, 2014; Wang *et al.* 2008).

Owing to the fact that synthetic dyes cause considerable damage to the flora and fauna of the ecosystem, several methods viz: precipitation, coagulation, reverse osmosis, ion-exchange, adsorption are adopted, but they fail to meet the requirements in two aspects cost-effectiveness and recycling nature (Marti *et al.* 2008; Liang *et al.* 2009; Gupta *et al.* 2015; Zare *et al.* 2015). Nevertheless, adsorption is found to be the most efficient and cost-effective method in the removal of trace amounts of dyes in the aqueous media (Sadegh *et al.* 2015a; 2015b; Gupta *et al.* 2015). Mesoporous materials, like activated carbon, zeolites, biomaterials, nanoparticles, polymers etc., are some adsorbents extensively used for adsorption of toxic dyes (Gupta *et al.* 2015; Zare *et al.* 2015; Sadegh *et al.* 2015a; 2015b; Gupta *et al.* 2015). Carbon nanotubes (Mahmoodian *et al.* 2014; Gupta *et al.* 2011; 2013a; 2013b; Nekouei *et al.* 2015; Ghaedi *et al.* 2015) and chemically modified polymers (Vidhyadevi *et al.* 2013; Murugesan *et al.* 2012; Kirupha *et al.* 2015), have attracted greater attention as adsorbents for the removal of dyes and metals because of their high adsorption capacity. Carbon nanotubes, they are unique in their structure and many outstanding mechanical, electronic and optical properties (Roberts *et al.* 1977), the adsorption capacity is considerably low. Researchers try to find out a better solution for the synthesis of CNTs with good adsorption capacity. SWCNTs and MWCNTs

**** Indiran Muralisankar***
email: imuralikavitha@gmail.com

were prepared using different techniques, such as evaporation, laser ablation, chemical vapor deposition, electrolysis and flame synthesis (Iijima, 1991; Das *et al.* 2014; Iijima and Ichihashi, 1993; Terrones, 2003; Farhat and Scott, 2006; Rafique and Iqbal, 2011). Some inorganic metals and organometallic complexes are used as catalysts in this method. The catalysts are generally made from metals or their salts (Nyamori *et al.* 2008). Pyrolysis is the most economical, cost effective methodology in synthesizing CNTs with source materials, which includes methane, acetylene, ethanol, benzene and polyvinyl alcohol (PVA) (Dikio *et al.* 2010; Dikio and Bixa, 2011; Benito *et al.* 2009; Liu *et al.* 2003; Shao *et al.* 2000; Jin *et al.* 2007).

The present study describes a simple synthesis of nickel oxide impregnated carbon composite (NiO-CNC) synthesized by burning paraffin wax along with nickel acetate by controlled pyrolysis methodology and its use as adsorbent for its effectiveness towards the removal of Congo red (CR) anionic dye, in aqueous medium. The effect of experimental parameters which influence the sorption process such as contact time (t), solution pH of the dye solution, initial dye concentration, adsorbent dose and temperature (T) has been investigated. Adsorption isotherms and kinetics were applied to different isotherm models to find out the best fit model which describe the sorption process and the mechanism involved with the obtained experimental data .The thermodynamic parameters Enthalpy change ($\Delta H°$), Gibbs free energy ($\Delta G°$) and Entropy change ($\Delta S°$), are calculated with the obtained results.

2. MATERIALS & METHODS

Nickel acetate (Ni $(CH_3CO_2)_2$) (Sigma-Aldrich), Paraffin wax (MERCK), Congo red (LABCHEM) are used as such without purification for synthesis and adsorption study. All working solutions for adsorption studies were prepared using de-ionized water with error deviation of less than ±1%.

2.1 Analytical methods

The X-ray diffraction patterns of NiO-CNC, were recorded using a Bruker AXS D8 advance diffractometer with Cu-Ka radiation. The surface morphology, composition and particle size were analyzed using a Leo Gemini 1530 Scanning Electron Microscope (SEM) at an accelerating voltage of 15kV with Energy dispersive studies (EDS) and Transmission electron microscopy (TEM, JEOL model JEM 2011) at an accelerating voltage of 200 KV. Raman spectra of NiO-CNC were recorded using the Renishaw in micro-Raman spectrometer, using an argon laser excitation wavelength of 514 nm at 20 mW powers with an illumination spot of size 1 µm and acquisition time 90 s. The concentration of the dye solution before and after adsorption experiments were measured using UV-Visible spectrophotometer (Shimadzu, Japan).

2.2 Synthesis of Nickel oxide activated carbon nanocomposite (NiO-CNC)

The mixture of precursors 35.7g of nickel acetate (Ni $(CH_3CO_2)_2$) (Sigma-Aldrich) and 36.7g paraffin wax (MERCK) (fused) were ground well in an agate mortar and taken in a china dish(4" dia). The mixture was lighted to give a bright orange lean flame. In order to avoid oxidation of carbon, the china dish with the burner was surrounded by a perforated card board for flame enhancement. The soot particles were collected in an inverted glass collector, the inner walls of which had been wetted by benzene previously. A continuous bright flame is maintained till all the wax is completely utilized. A schematic diagram for collecting NiO-CNC is shown in Fig. 1. The entire process took about 2 hr. Then the porcelain tile collector with NiO-CNC was scratched mechanically by a wooden spatula to collect the product, which was then stored in a desicator.

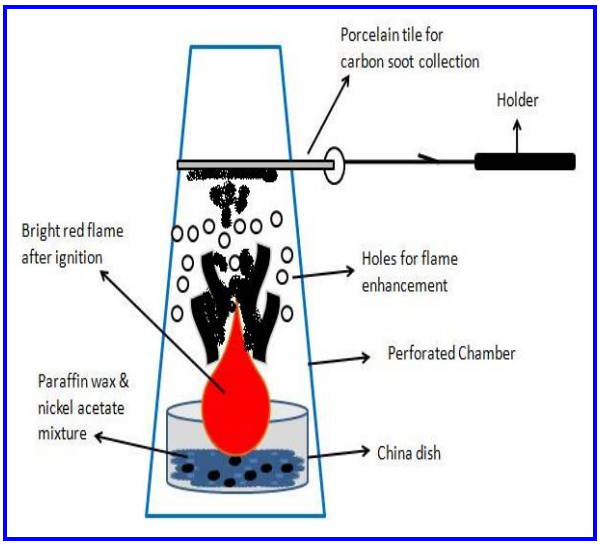

Fig. 1: Schematic diagram for the formation of nickel oxide carbon nanocomposite (NiO-CNC) using pyrolysis method

2.3 Preparation of Congo red (CR) dye solution

Adsorption experiments were carried out with 250 mL conical flask using 100 mL of CR dye solution. 20 mL of desired concentration of dye solution is taken

along with appropriate amount of NiO-CNC adsorbent for complete adsorption to take place at 180 rpm agitation speed for a required time. The parameters influencing adsorption process were varied for each trial, such as solution pH (2 to 11), initial dye concentration (20, 40, 60, 80 and 100 mg/L), adsorbent dose (20, 40, 60, 80, 100 mg), contact time (0, 10, 20, 30, 40, 50 and 60 min.) and temperature (303, 313, 323 and 333K). After completion of each adsorption experiment, the samples were centrifuged and the concentration of the supernatant solution were analyzed using UV double beam spectrophotometer at wavelength λ= 498 nm. All parameters were optimized separately, using the same procedure.

The percentage removal of the dye solution (R) and the adsorption capacity q_e was calculated using the equation (1) and (2);

$$R = \frac{(C_o - C_e)}{C_o} \times 100 \quad (1)$$

$$q_e = \frac{V(C_i - C_t)}{m}, \quad (2)$$

where C_o is the initial dye concentration (mg/L), C_e is the concentration of dye solution at equilibrium and C_t is the concentration of the dye solution at time (t), V is the volume of dye solution (L) and m is the amount of NiO-CNC (g). All the experiments were repeated thrice and their average was taken with minimum error (SSE±2).

3. RESULTS & DISCUSSION

3.1 Characterization of Nickel oxide activated carbon nanocomposites

The low and high resolution SEM images of NiO-CNC are shown in fig.2a and 2b respectively. The former image depicts the cluster of tubular and spherical carbon particles of 51.28 nm. The latter, a high solution image of the former, indicates a carbon tubes incorporated with bright particles of oxide of size 50 nm approximately, at their walls.

The TEM image micrographs are shown in Fig. 3(a-d) respectively. From Fig. 3(a), it is inferred that spherical particles are interconnected through carbon nanotubes resulting in the formation of clusters. The bridging of nanotubes results in the formation of nanosphere with nickel oxide present inside it. The overlapping of nanosphere results in the formation of CNT in which the nanosphere itself acts as a self-catalyst. It shows the carbonaceous material soot at 200 nm and the nanomaterial obtained on burning paraffin wax is of spherical nature, NiO is embedded on the pores of the carbon matrix. The lattice fringe describes the graphene layers of the carbon nanosphere, which are observed in Fig. 3(c). The fringes are found to be non-uniform and crystalline is reflecting the graphitization of the nanospheres. With the appearance of diffraction rings and bight spots in the SAED patterns show clearly the high degree of crystalline nature of the particles (Shooto and Dikio, 2011). The presence of pure carbon and nickel atoms can be seen clearly from the X-ray EDX analysis spectrum in Fig. 3(d) without any contamination under permissible limit (±0.01).

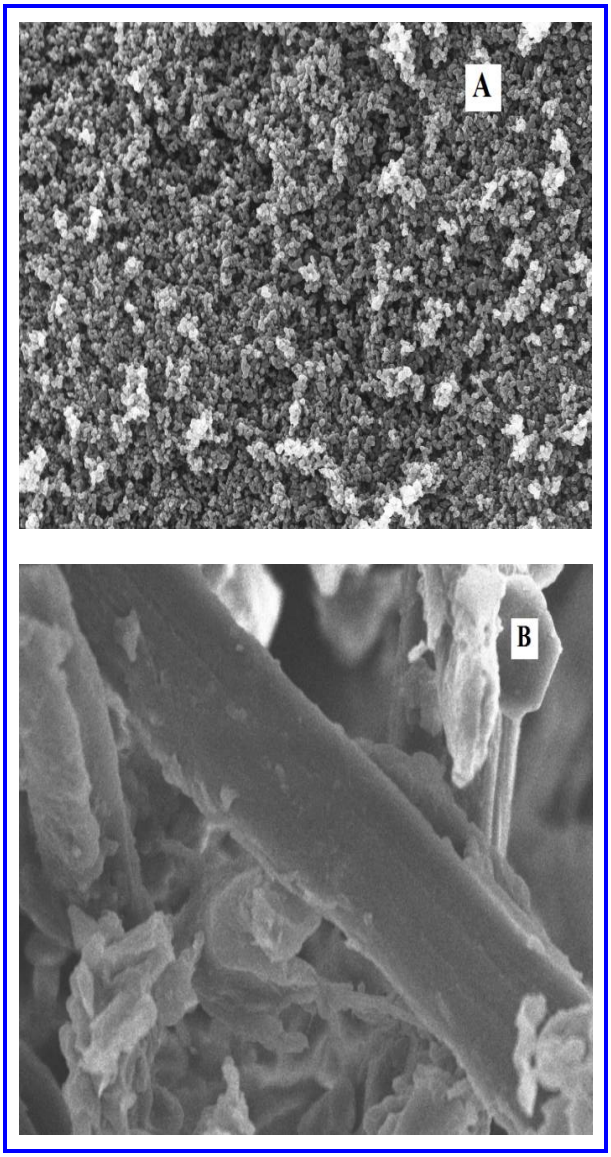

Fig.. 2: Field Emission Scanning Electron Microscopy (FE-SEM) of NiO-CNC (A); Higher Magnification imaging of single CNT wrapped with NiO (B)

3.2 Size and Textural morphology

The peaks at 37.26°, 43.90°, 64.28° and 77.41° correspond to (111), (200), (220) and (222) planes, (JCPDS card No :47-1049) as a justification for the presence of NiO in NiO-CNC (Fig. 4). A broad peak between 20° to 30° plane indicates the presence of the hexagonal lattice of multi-walled carbon nanotubes (MWCNT) with the deposition of amorphous carbon (Langmuir, 1918; Freundlich, 1906; Adamson, 1997). The particle size of NiO-CNC is 50-58 nm in diameter calculated using the Scherer's equation.

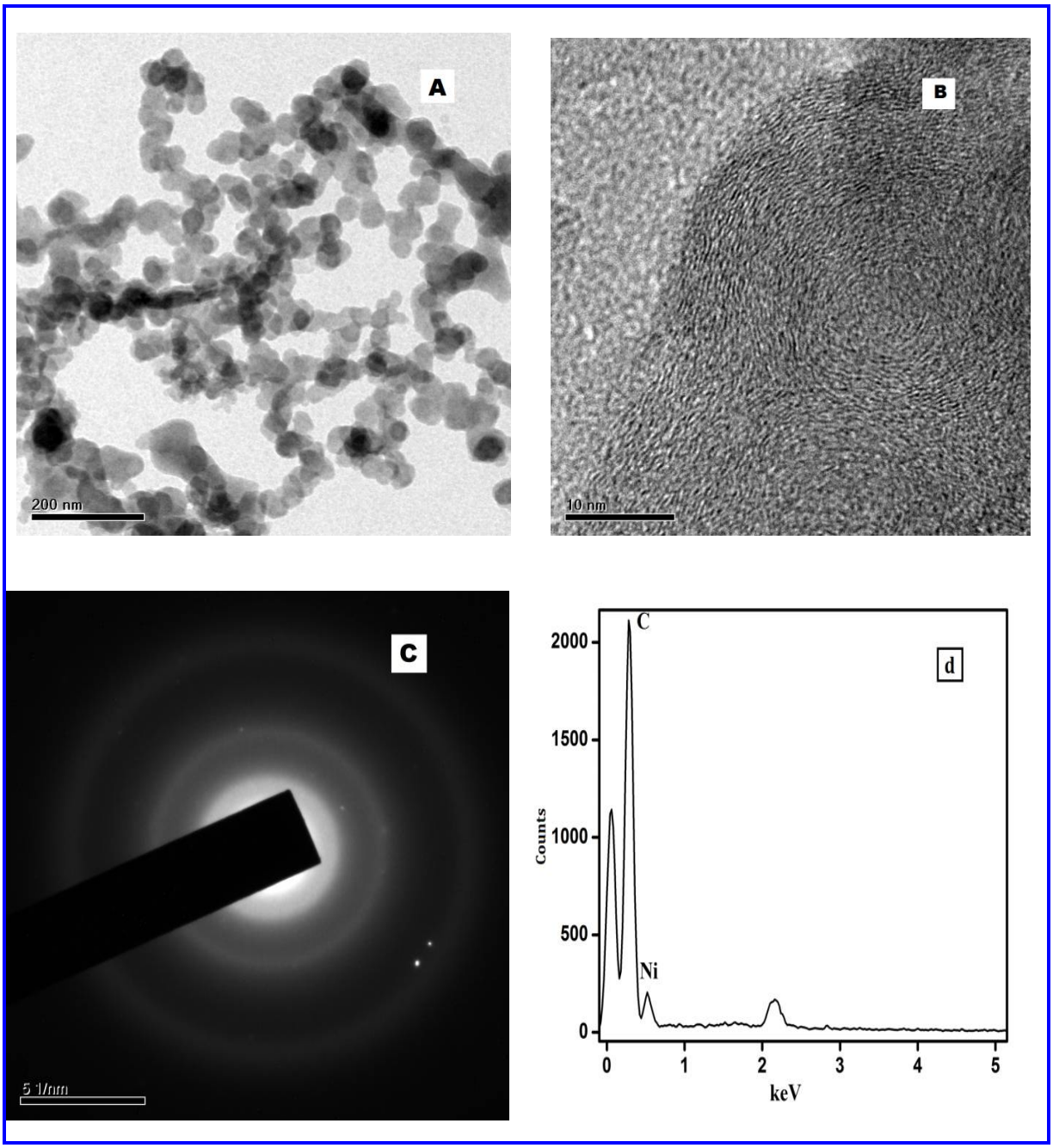

Fig. 3: TEM imaging of NiO-CNC (a); Higher Magnification Imaging of NiO-CNC (b); SAED patterns of NiO-CNC (c); EDAX spectra of NiO-CNC (d)

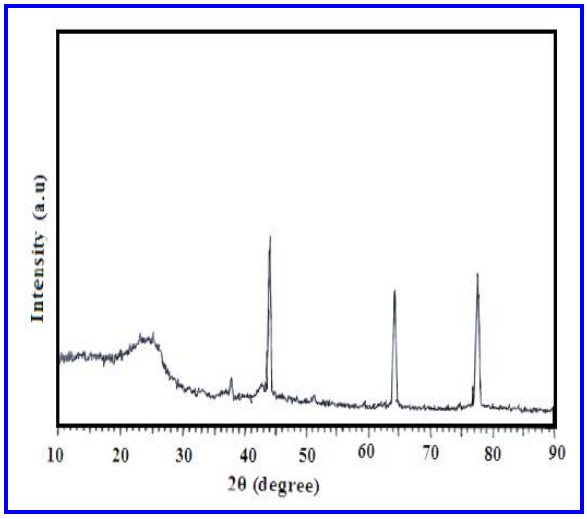

Fig. 4: XRD spectrum of NiO-CNC adsorbent

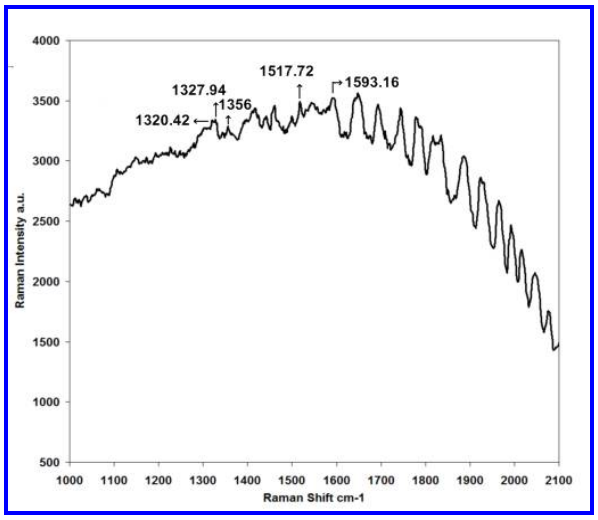

Fig.. 5: Raman Spectrum of NiO-CNC adsorbent

The Raman spectrum of NiO-CNC is given in Fig. 5 with the range between 1000cm^{-1} to 2100 cm^{-1}. The peaks observed at 1310 cm^{-1} and 1605 cm^{-1} correspond to the D-band and G-band respectively. The D band is a breathing mode that depicts the disordered structures and edge planes as it is forbidden in perfect single graphene layer. The D-band originates from the disorder in sp^2-hybridized carbon, thereby signifying the lattice distortions in curved graphene sheets and spheres etc. Apparently in the present study, the distortion is low due to the presence of sp^3-hybridized carbon. The G band corresponds to the scattering of E_2g mode of the sp^2 atoms, with high intensities assigned to phonon mode of the graphite single layer seen in all the samples suggesting that NiO-CNC is composed of crystalline graphitic carbon.

3.3 Sorption Experimental study

3.3.1 Effect of time dependant factor and solution pH onto CR sorption

The influence of time dependant behavior of CR dye sorption onto NiO-CNC was examined by varying the contact time (0-60 min.) taking 20 ppm initial CR dye solution with 0.05g of sorbent. There is a steady increase in dye removal with increase in time (Fig 6). It was observed that 80% of dye removal was attained in 15 min. and a maximum removal of 96% was obtained in 60 min., after which no further change was observed. Hence the optimized time of 60 min. was selected for further studies. This is due to the fact that there were large numbers of vacant sites readily available for adsorption in 15 min and after that, the vacant sites were reduced gradually up to 60 min and then there existed a repulsive force of attraction between the absorbed dye molecules on the NiO-CNC surface and solid phase (Dubinin and Radushkevich, 1947).

One of the most significant parameters which influence the amount of CR dye removal by NiO-CNC is solution pH. The influence of CR dye removal by NiO-CNC surface was analyzed with pH ranging 2-11, using initial concentration of 20ppm dye solution with 0.05 gm of NiO-CNC dose under 60 min. (optimized) of contact time. With increase in pH, the adsorption increased gradually and reached maximum at pH-11. Maximum adsorption of 96.87 mg/g was obtained for CR removal using NiO-CNC adsorbent (Fig. 6).

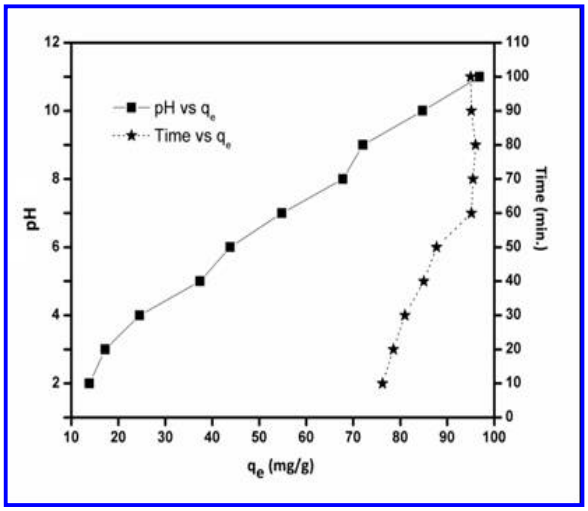

Fig.. 6: Effect of solution pH and Time dependant factor on CR removal by NiO-CNC. (Initial CR dye concentration: 100 mg/L, NiO-CNC dose: 20 mg, sample solution: 20 mL, Variable time period: 0-60 min., Variable Solution pH: 2-11 and temperature: 30 °C)

The pH dependency of adsorption efficiency could be explained by the functional groups involved in dye uptake and dye chemistry. Maximum dye removal was attained in the basic medium at a pH 11. Formation of hydroxide dominates, leading to the binding interaction with the competition between Ni^{2+} of the adsorbent and Na^{+} ion in the dye resulting in the formation of NaOH predominates. This led to the replacement of Ni^{2+} over Na^{+} that was clearly explained in the mechanism. A comparism of sorption isotherms of CR onto various sorbents are listed in Table 1

Table 1. Comparison of sorption isotherm onto various sorbents

Adsorbents	Isotherm	q_e (mg/g)	References
Chitosan hydro beads	Langmuir	92.59	Chatterjee *et al.* 2007
Coal-based Activated carbon	Langmuir	52	Grabowska and Gryglewicz, 2007
Cashew nut shell	Langmuir	5.18	Kumar et al. 2010
Cashew nut shell	Freundlich	1.35	Kumar et al. 2010
Kaolin	Fruendlich	1.98	Vimonses *et al.* 2009
Raw pine cone	Freundlich	19.18	Dawood and Sen, 2012
Acid-treated pine cone	Experimental	40.19	Dawood and Sen, 2012
NiO-CNC	Langmuir	95.02	Present Study

3.3.2 Effect of initial dye concentration and sorbent amount onto CR sorption

The influence of initial CR concentration using NiO-CNC was studied and represented in Fig. 7. From the experimental results obtained for CR removal using NiO-CNC with varying CR dye concentration (20-100 mg/L) with adsorbent (0.05 g), it was understood that rapid removal occurred in the initial stage, due to the binding of CR dye more number of sites available for adsorption. At equilibrium, saturation occurs due to the complete occupation of sites on adsorption.

The amount of NiO-CNC adsorbent amount also plays a vital role in deciding the cost-effectiveness of the process. The effect of NiO-CNC dose onto CR dye removal is shown also in Fig. 7. It is evident from the figure, that the increase in CR dye is rapid with increase in NiO-CNC amount. But, no change was observed beyond the dose of 5g/L. This is because of the absence of available sites and exchanging of ions in the adsorption process.

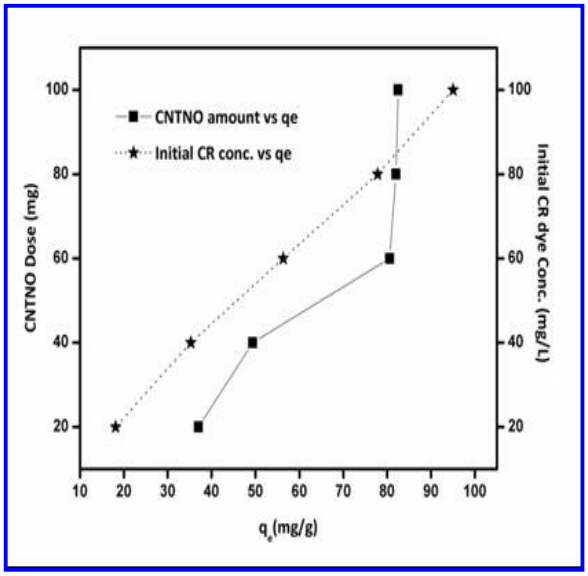

Fig. 7: Effect of NiO-CNC dose and initial concentration of CR removal by NiO-CNC (Solution pH: 11, equilibrium time: 60 min., Sample solution: 20 mL, Variable Initial CR concentration: 20-100 mg/L, Variable NiO-CNC dose: 20 -100 mg and temperature: 30°C)

3.4 Sorption isotherm

A sorption isotherm is a relationship between equilibrium sorption capacity and equilibrium concentration at a certain temperature. To determine the sorption capacity of NiO-CNC and design of the process, isotherms were obtained at 303K, 313K, 323K and 333K, respectively. q_e is the sorption capacity (mg/g); C_e is the equilibrium concentration (mg/L). A plot of C_e verses q_e is plotted with 2-parameter and 3-parameter non-linear isotherm models using MATLAB 7.1 to find out the most best suitable fitting model. The experimental data were plotted with 2-parameter models: Langmuir (1918) and Freundlich (1906), Temkin (1940) and Dubinin - Radushkevich (1947) and 3-parameter model: Redlich-peterson (1959), Sips (1948), Khan (1997) and Toth (1971) models (Fig 8 & 9(A-D)) The parameter constants, co-relation co-effecients, sum of error squared (SSE) and root mean square (RMSE) were summarized (Table 1.)

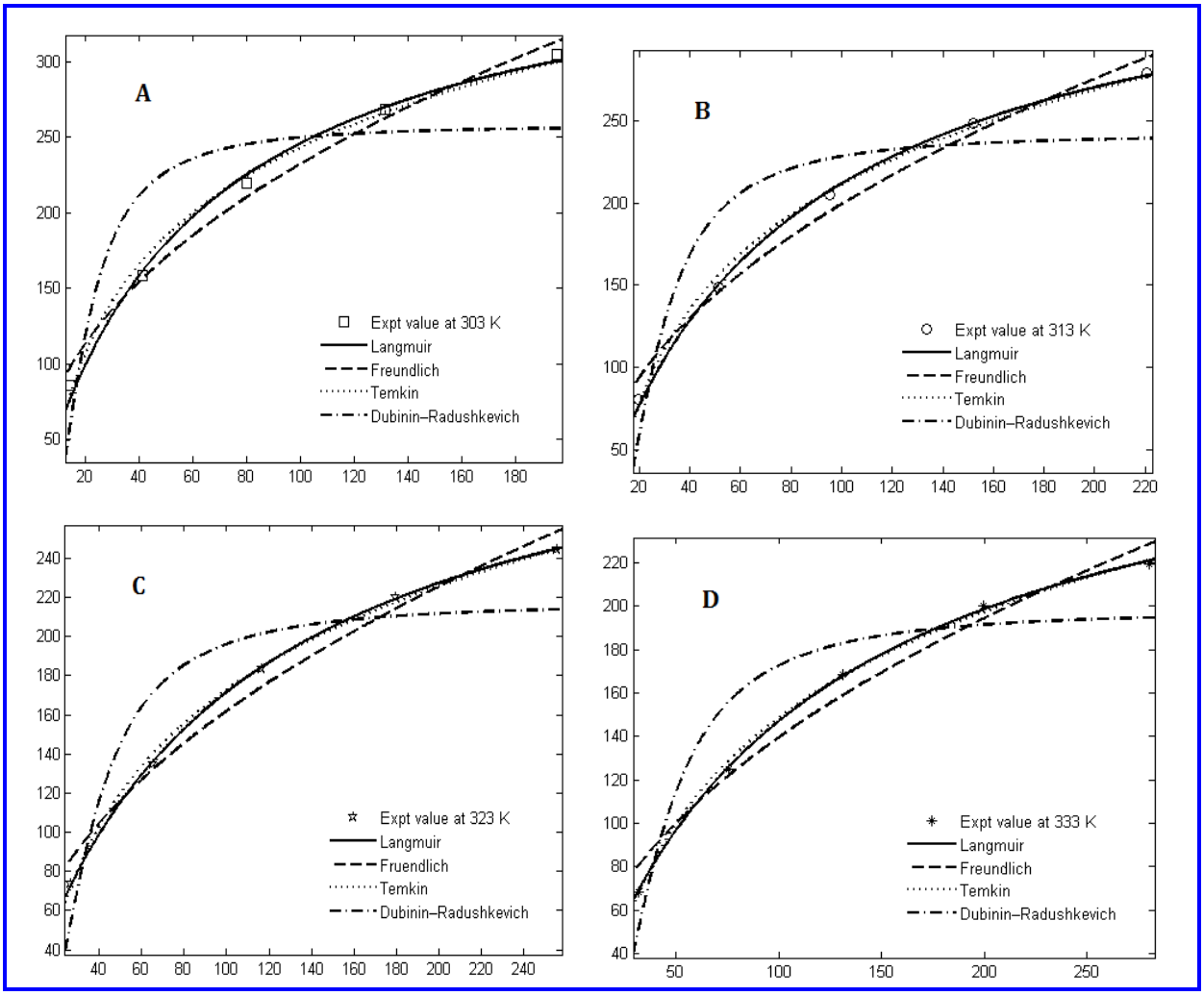

Fig. 8(A-D): Non-linear 2-Parameter isotherm model of NiO-CNC sorbent with temperature variation gradient.

3.4.1 Two-Parameter isotherm Model

An assumption of maximum sorption occurs when a saturated monolayer of the solute molecules binds with the surface of the sorbent, no migration of sorbate molecule on the surface plane and the sorption energy is constant. The non-linear form of the Langmuir isotherm model (1918) is expressed as follows

$$q_e = \frac{q_{max} b_L C_e}{1 + b_L C_e} \qquad (3)$$

where q_e is the amount of metal adsorbed (mg/g), and C_e is the equilibrium concentration of the solution (mg/L). q_m and b_L are the Langmuir constants indicating the adsorption capacity and energy, respectively. The essential feature of the Langmuir model can be expressed in terms of a dimensionless constant separation factor (R_L);

$$R_L = 1/1+(1+K_L C_o) \qquad (4)$$

where K_L is the Langmuir constant (L/mg) and C_o is initial concentration (mg/L).

Freundlich isotherm (1906) is the earliest known relationship describing the non-ideal and reversible adsorption, not restricted to the formation of monolayer. This empirical model can be applied to multilayer adsorption, with non-uniform distribution of adsorption heat and affinities over the heterogeneous surface (Adamson and Gast, 1997). The non-linear form of Freundlich isotherm is represented as

$$q_e = K_f C_e^{1/n} \qquad (5)$$

where K_F is the Freundlich isotherm constant ((mg/g). n=adsorption intensity, Ce= equilibrium concentration of adsorbate (mg/L) , q_e = the amount of metal adsorbed of the adsorbent at equilibrium.

The Temkin isotherm (1940) model describes explicitly about the adsorbent–adsorbate interactions. This model assumes the following conditions: (i) the heat of adsorption of all the molecules in the layer decreases linearly with the coverage due to adsorbent–adsorbate interactions, and that (ii) the adsorption is characterized by a uniform distribution of binding energies, up to some maximum binding energy. The derivation of the Temkin isotherm assumes that the fall in the heat of sorption is linear rather than logarithmic, as implied by the Freundlich equation. The non-linear form of Temkin isotherm is represented as

$$q_e = B_T \ln(AC_e) \quad (6)$$

where B_T = RT/b, is the constant related to the heat of adsorption, b is the heat of adsorption (kJ/mol), R is the gas constant (8.314 J/mol.K), T is the temperature (K) and A is the adsorption equilibrium binding constant related to the maximum binding energy (L/mg).

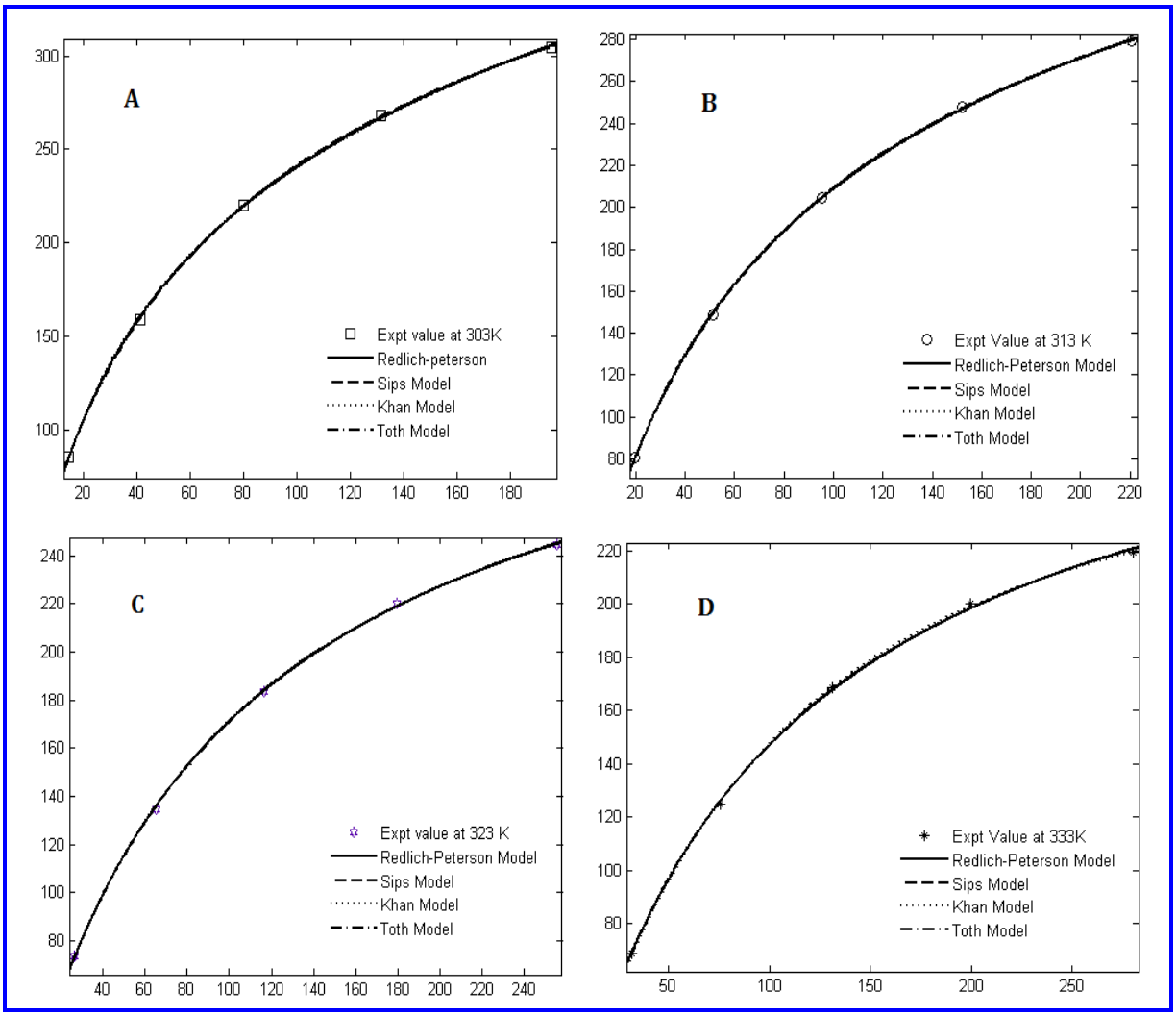

Fig. 9(A-D): Non-linear 3-Parameter isotherm model of NiO-CNC sorbent with temperature variation gradient

Dubinin-Radushkevich isotherm (1947) is an empirical model initially conceived for the adsorption of subcritical vapours onto micropore solids following a pore filling mechanism. It is generally applied to express the adsorption mechanism (Gunay, 2007) with a Gaussian energy distribution onto a heterogeneous surface (Dabrowski, 2001).The non-linear form of Dubinin-Radushkevich isotherm is represented as

$$q_e = q_m \exp\left(-\beta\left(RT \ln\left(1+\frac{1}{C_e}\right)\right)^2\right) \quad (7)$$

where q_e = amount of adsorbate in the adsorbent at equilibrium (mg/g), Ce= equilibrium concentration of adsorbate (mg/L) qm is the Dubinin–Radushkevich monolayer capacity (mg/g), β is a constant related to sorption energy (mean free energy), R is the gas constant (8.314 J/mol K) and T is the absolute temperature.

$$E = \frac{1}{\sqrt{2\beta}} \quad (8)$$

The magnitude of E is used to determine the type of adsorption mechanism; When one mole of ions is transferred to the adsorbent surface, its value is less than 8 kJ/mol which indicates the physical adsorption (Benito, 2009). The value of E is between 8 and 16 kJ/mol, which indicates the adsorption process follows ion- exchange (Liu *et al.* 2003), while its value in the range of 20–40 kJ/mol indicates chemisorption (Shao *et al.* 2000).

From the (theoretical) q_{max} value was found to be almost similar to the experimental value obtained from the studies. The adsorption process is found to be exothermic, the q_e values are found to be in the decreasing order with increase in temperature gradient. The R^2 values of Langmuir isotherm of in the order of 0.9956, 0.9986, 0.9998 and 0.9996 with increase in temperature from 30°C, 40°C, 50°C and 60°C stating the Langmuir isotherm fits well with the obtained equilibrium data. The value of n > 1, from Freundlich isotherm indicates that, the process is a physical adsorption. The values of A and B constants of Temkin isotherm are in the range of 0.1-0.08 and 36-30 in the decreasing order with increase in temperature. The Dubinin–Radushkevich isotherm value, q_m is 258.1 mg/g, β is 9.97×10^{-8} mg^2/J^2 and the magnitude of E = 22.34 of at 30 °C indicating that reaction follows chemisorption. Finally, suggesting that both physical adsorption and chemical adsorption takes place simultaneously, which results in the increased dye removal by the adsorbent NiO-CNC. The Non-linear isotherm parameters obtained using 2-parameter models with temperature gradient are listed in Table 2.

Table 2. Non-linear isotherm parameters obtained on CR removal using NiO-CNC using 2-parameter models with temperature gradient

2-Parameter Isotherm model	Parameters & constants	Congo red removal			
		30 °C	40 °C	50 °C	60 °C
Langmuir	q_m (mg/g)	390.6	373.1	337.6	305.9
	k_L(L/mg)	0.01701	0.01312	0.01033	0.00925
	R^2	0.9956	0.9986	0.9998	0.9996
	SSE	133.2	34.82	3.609	6.417
	RMSE	6.664	3.407	1.097	1.463
Freundlich	K_f [(((mg/g)(L/mg)(1/n))]	29.55	23.14	17.8	15.38
	n (g/L)	2.234	2.14	2.086	2.088
	R^2	0.9885	0.9853	0.9805	0.9757
	SSE	349.5	369.9	366.8	358.2
	RMSE	10.79	11.1	11.06	10.93
Temkin	A (constant)	0.1765	0.128	0.09533	0.08253
	B (constant)	36.77	35.95	33.25	30.55
	R^2	0.9943	0.9963	0.9978	0.998
	SSE	173.9	93.8	41.66	28.77
	RMSE	7.614	5.592	3.726	3.097
Dubinin-Radushkevich	q_m (mg/g)	258.1	242	217.2	198.1
	B (mg^2/J^2)	0.000997	0.001792	0.003127	0.004209
	R2	0.7715	0.8026	0.8343	0.8541
	E	22.37	17.06	12.64	10.9
	SSE	6974	4977	3114	2152
	RMSE	48.22	40.73	32.22	26.78

3.4.2 Three-Parameter Model

Redlich-Peterson isotherm (1959) is a combination of Langmuir and Freundlich models. It approaches the Freundlich model at higher concentration and is in accordance with the lower concentration limit of the Langmuir equation. The non-linear form of Redlich-Peterson isotherm model is as follows,

$$q_e = \frac{K_R C_e}{1 + \alpha_R C_e^{\beta}} \quad (9)$$

where q_e is the amount of adsorbate in the sorbent at equilibrium (mg/g), C_e is the equilibrium concentration (mg/L); K_R is the Redlich - Peterson isotherm constant (L/g), α_R is the Redlich - Peterson isotherm constant (L/mg), and β is the exponent, which lies between 0 and 1; if β nearer to 1, Langmuir isotherm will be preferable and if β is nearer to 0, Freundlich is preferable.

Sips isotherm (1948) is a combined form of Langmuir and Freundlich expressions deduced for predicting the heterogeneous adsorption systems (2007) and circumventing the limitation of the rising adsorbate concentration associated with Freundlich isotherm model. At low adsorbate concentrations, it reduces to Freundlich isotherm. At high concentrations, it predicts a monolayer adsorption capacity characteristic of the Langmuir isotherm. The non-linear form of Sips Model is expressed as

$$q_e = \frac{q_m K_s C_e^{n_s}}{1 + a_s C_e^{n_s}} \quad (10)$$

where K_s is the equilibrium constant, if the value of n_s is equal to 1 then this equation will become a Langmuir equation. Alternatively, as either C_e or a_s approaches 0, the isotherm follows Freundlich model.

Khan isotherm model (1997) is generally suggested for pure solutions. The non-linear form of Khan Model is expressed as

$$q_e = \frac{(q_m b_k C_e)}{(1 + b_k C_e)^{a_k}} \quad (11)$$

where b_K is the Khan model constants and a_K is the Khan model exponent.

Toth isotherm model (1971) is another empirical equation developed to improve Langmuir isotherm fittings (experimental data), and useful in describing heterogeneous adsorption systems, satisfying both low and high-end boundary of the concentration (2006). The non-linear form of Toth Model is expressed as

$$q_e = \frac{F b_T C_e}{\left[1 + (b_T C_e)^{1/n}\right]^n} \quad (12)$$

b_T is the Toth model constant and n is the Toth model exponent ($0 < n \leq 1$).

The exponents, constants and parameter values are given in Table 3 with temperature gradient. From the results, sorption takes place effectively at room temperature suggesting the sorption is more feasible and exothermic. The Redlich-Peterson parameters K_R value is 9.417 (L/g), α_R is 0.0702 (L/mg) and B_R is 0.8106 nearer to 1, indicating that Langmuir fits well with the obtained experimental data. The values from the sips isotherm, a_s and n_s are 0.0098 and 0.7834 respectively. Since the value of n_s approaches 1 indicating Langmuir isotherm fits well. The q_{max} value from Khan Model is 191.8 mg/g. The constants a_k and b_k are 0.7453 and 0.0440. The value of F is 578.6 mg/g and constants b_T and n are 9.624, 0.5807, respectively.

3.4.3 Comparison of isotherms

Considering the relative errors, parameters and the constants from the 2-Parameter and the 3-Parameter isotherm models, th R^2 values are in the range of Langmuir > Temkin > Freundlich > Dubinin-Radushkevich and in the case of 2-Parameter isotherm models and in 3 parameter isotherm models Toth > Sips > Redlich-Peterson > Khan. However, the results of the non-linear regression analysis indicate that the 3-Parameter isotherm model has no noticeable change in the CR-NiO-CNC sorption system. Correlation of the experimental data with these isotherm models implies that both monolayer and heterogeneous surface exist under the experimental conditions studied. Langmuir isotherm fit well suggesting that the dye molecules binds on the pores and walls of the nanosphere with physorption as the predominating mechanism along with the chemical interaction suggesting that the adsorption mechanism is complex.

3.5 A Single Stage Batch Adsorber Design

The best fitted adsorption isotherm model was utilized to outline the batch adsorber for the expulsion of dye from dye solution. The schematic perspective of the batch adsorber was appeared in Fig. 10. The plan goal of the present adsorber was to quantify the measure of adsorbent which is requirement for treating the known volume and concentration of the CR dye from the aqueous at ideal condition. The material balance for the batch adsorber is given as follows:

$$V\,(C_o - C_e) = M(q_e - q_o) \qquad (13)$$

where V is the volume of copper ions solution (L), Co is the initial copper ions concentration (mg/L), C_e is the copper ions concentration at equilibrium (mg/L), M is the mass of the adsorbent (g), q_e is the equilibrium adsorption capacity (mg/g), q_o is the adsorption capacity at time t = 0 (mg/g). The fresh adsorbent was used for the present adsorption system, so, the $q_o = 0$ and the Eq. (13) can be rewritten as:

$$M = \frac{(C_o - C_e)}{q_e} V \qquad (14)$$

Table 3. Non-linear isotherm parameters obtained on CR removal using NiO-CNC using 3-parameter models with temperature gradient

3-Parameter Isotherm Models	Parameters and constants	Congo red removal			
		303K	313K	323K	333K
Redlich-Peterson Model	K_{RP} (L/g)	9.417	5.822	3.56	2.831
	α_{RP} (L/mg)	0.0702	0.03094	0.011 74	0.009256
	β_{RP}	0.8106	0.8809	0.9817	1
	R^2	0.9998	0.9998	0.9998	0.9996
	SSE	6.161	4.159	3.184	6.417
	RMSE	1.755	1.422	1.262	1.463
Sips Model	K_s $(mg/L)^{-1/n}$	12.77	7.41	3.824	2.831
	β_s	0.7834	0.8728	0.9736	1
	a_s	0.0098	0.009698	0.009794	0.009256
	R^2	0.9999	0.9999	0.9999	0.9996
	SSE	0.7209	1.18	2.631	6.417
	RMSE	0.6004	0.7681	1.147	1.463
Khan Model	Q_{max} (mg/g)	191.8	244.4	321.4	305.9
	b_k	0.04403	0.02248	0.01096	0.009256
	a_k	0.7453	0.8209	0.9746	1
	R^2	0.9997	0.9998	0.9998	0.9998
	SSE	10.18	6.056	3.373	2.4
	RMSE	2.256	1.74	1.299	1.095
Toth Model	F (mg/g)	578.7	455	347.7	308.4
	g	9.624	23.89	77.34	100
	d	0.5807	0.7424	0.9522	0.9845
	R^2	0.9999	0.9999	0.9998	0.9995
	SSE	2.545	2.395	2.926	7.249
	RMSE	1.128	1.094	1.21	1.554

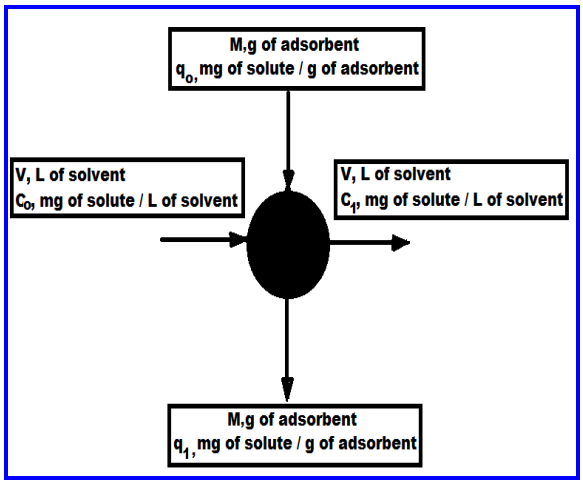

Fig. 10: Single-stage batch adsorber design

The best obeyed adsorption isotherm show for the present adsorption framework was the Langmuir model. This model was incorporated into the Eq. (14) and the condition can be changed as:

$$M = \frac{(C_o - C_e)(1 + K_L C_e)}{q_m K_L C_e} V \qquad (15)$$

The Eq. (15) relates the mass of adsorbent with the volume of the CR dye solution for the initial concentration of dye solution at a constant temperature. The adsorption isotherm information was fitted to the Eq. (15) and the outcomes are appeared in Fig. 11.

3.6 Sorption Kinetics

Several models were proposed to express the mechanism between the solute sorption onto the sorbent. To investigate the mechanism of sorption by NiO-CNC onto CR dye removal, parameter constants were calculated using the pseudo first order (Sips, 1948), pseudo second order (Gunay, 2007), Elvolich equation (Khan *et al.* 1997) and Intra-particle diffusion (Toth, 1971). The linear form of pseudo first order model (Eqn. 16) is as follows,

$$\text{Log } (q_e - q_t) = \log q_e - K_{1\text{-ad}}\, t / 2.303 \qquad (16)$$

where $K_{1\text{-ad}}$, q_t and q_e are the pseudo first order equilibrium rate constant (1/min), amount of dye adsorbed at time t (mg/g) and amount of CR dye adsorbed at equilibrium time t (mg/g). Linear plot of ln (q_e-q_t) against contact time t is plotted. (Fig 12).

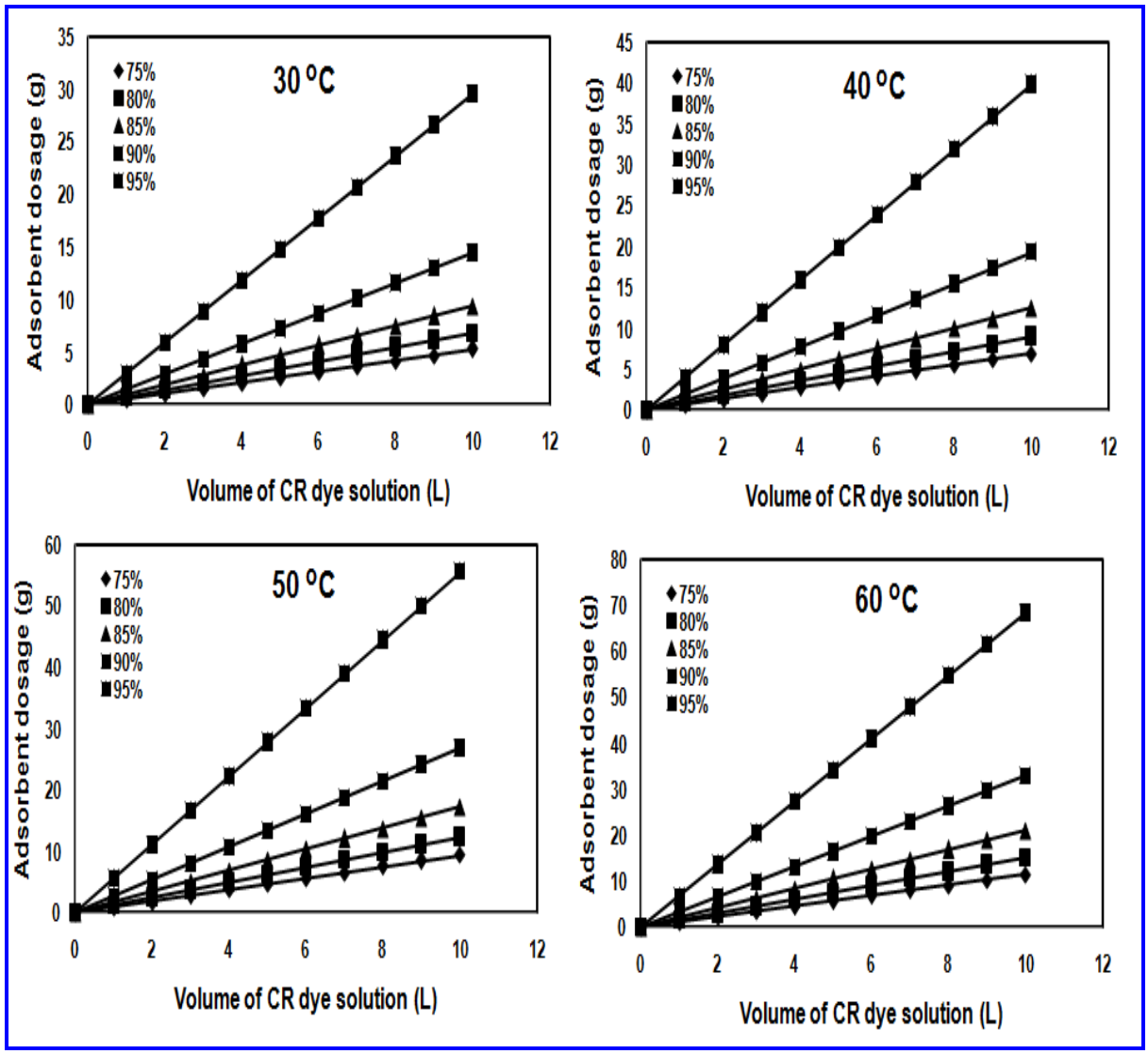

Fig. 11: Adsorber design results for the removal of CR dye by NiO-CNC

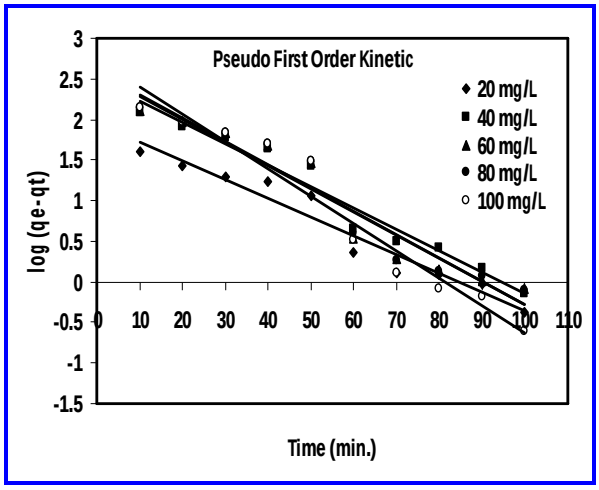

Fig. 12: Pseudo-first order kinetic model of NiO-CNC onto CR removal with concentration gradient at 30 °C

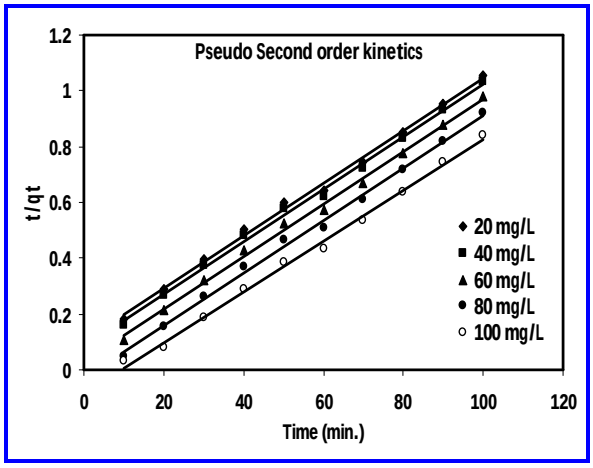

Fig. 13: Pseudo-second order kinetic model of NiO-CNC onto CR removal with concentration gradient at 30 °C

The linear form of the pseudo-second order model (Eqn. 17) is as follows

$$\frac{t}{q_t} = \frac{1}{k_2\, q_e^2} + \frac{1}{q_e} t \qquad (17)$$

where k_2 is the pseudo-second order sorption rate constant (g/(mg.min)), q_e and q_t are defined as same above. A linear plot of t/qt against t is plotted. (Fig. 13) .

From the studies, it was clearly evident that the reaction follows pseudo-second order kinetic from the values of co-relation co-coefficient R^2 ≥0≤1. The experimental sorption capacity q_e values fits well close to the observed theoretical one. From the obtained rate constants and parameter constants shown in Table 4 confirms that the pseudo-second order model is a good fit in the adsorption process.

3.6 Thermodynamic Test

The thermodynamic parameters, such as standard free energy change (ΔG°), enthalpy change (ΔH°) and entropy change (ΔS°) have been estimated to evaluate the feasibility of the adsorption process.

$$K_c = \frac{C_{Ae}}{C_e} \qquad (18)$$

$$\Delta G^o = -RT \ln K_c \qquad (19)$$

$$\log K_c = \frac{\Delta S^o}{2.303R} - \frac{\Delta H^o}{2.303RT} \qquad (20)$$

where K_c is the adsorption equilibrium constant, C_{Ae} is the amount of metal ions adsorbed onto the adsorbent per liter of solution at an equilibrium (mg/L), C_e is the concentration of metal ions in the solution at an equilibrium (mg/L), R is the gas constant (8.314 J/mol K) and T is the temperature (K). The observed thermodynamic data for the removal of CR dye using NiO-CNC is made to fit with the equations (18) and (19). A plot of K_c against 1/T is plotted (Fig. 14) and the results are tabulated (Table 5). The values are found to be decreasing with increasing in temperature indicating the adsorption process is more feasible at low temperature. The negative (ΔG) values indicate that, the adsorption process is more feasible and spontaneous. The negative (ΔH) value indicates the process is exothermic system and entropy change (ΔS) indicates the adsorption process is randomness at CR/NiO-CNC interface.

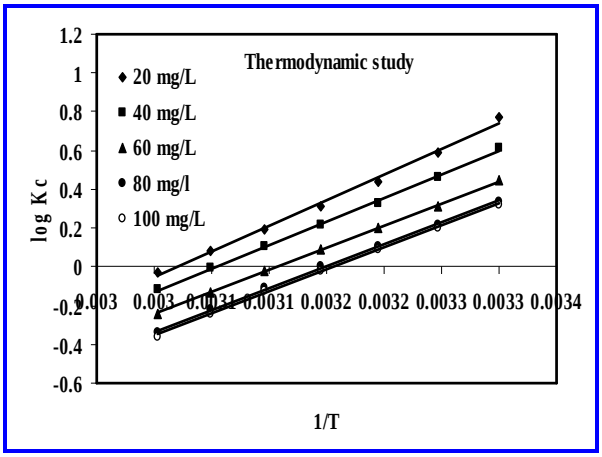

Fig. 14: Van-Hoff plot for thermodynamic studies on CR removal

Table 4. Kinetic parameters and constants on CR removal using NiO-CNC at 30°C

Kinetic Model	Parameters	Initial concentration of CR dye solutions (mg/L)				
		20	40	60	80	100
Pseudo First Order Model	k_{ad} (min^{-1})	1.74×10^{-4}	1.99×10^{-4}	2.15×10^{-4}	2.18×10^{-4}	2.55×10^{-4}
	$q_{e,}$ cal (mg/g)	6.64	9.12	9.40	9.51	10.05
	R^2	0.9497	0.9622	0.9367	0.9363	0.9483
Pseudo Second Order Model	k ($g\ mg^{-1}min^{-1}$)	3.22×10^{-4}	3.21×10^{-4}	3.23×10^{-4}	3.19×10^{-4}	3.32×10^{-4}
	q_e cal ($mg.g^{-1}$)	14.38	31.8	49.78	69.25	91.89
	qe expt. ($mg.g^{-1}$)	18.12	35.26	56.31	77.83	95.02
	h($mg.g^{-1}.min^{-1}$)	9.727	12.30	34.36	32.36	11.97
	R^2	0.9968	0.9969	0.9961	0.9968	0.9960

Table 5. Thermodynamic parameters and constants of NiO-CNC sorbent at 30 °C

Congo red Conc. (mg/L)	ΔH^o (kJ/mol)	ΔS^o (J/mol/K)	ΔG^o (kJ/mol)						
			303 K	308 K	313 K	318 K	323K	328K	333K
20 mg/L	-50.55	-153.02	-1.950	-1.502	-1.139	-0.818	-0.518	-0.218	-0.0755
40 mg/L	-46.53	-142.11	-1.552	-1.183	-0.861	-0.563	-0.274	-0.023	0.032
60 mg/L	-43.76	-135.93	-1.120	-0.807	-0.516	-0.233	0.513	0.354	0.670
80 mg/L	-43.19	-135.96	-0.852	-0.562	-0.282	-0.002	0.287	0.602	0.941
100 mg/L	-43.22	-136.41	-0.797	-0.510	-0.232	0.048	0.338	0.657	1.002

4. CONCLUSION

The present study describes the synthesis of MWCNT using paraffin wax with the incorporation of NiO by using nickel acetate as catalyst by, the combustion process. The synthesized NiO wrapped MWNT was tested for the suitability as an adsorbent for the removal of Congo red dye in aqueous medium. The adsorption equilibrium parameters such as, solution pH, contact time, NiO-CNC dose and Initial CR dye concentration are evaluated to find out the optimized conditions for feasible nature of the process. The maximum removal of 80% is observed under pH of 11, dose of 5g/L and initial CR dye concentration of 100 mg/L, with time period of 60 minutes. The obtained equilibrium data fits well with the Langmuir model. The negative ΔG, ΔH and ΔS values, reporting the adsorption is feasible, exothermic and spontaneous. Over all results suggest that the MWCNT/ NiO are an effective and better adsorbent, when compared to the reported adsorbent for the removal of dyes from textile effluents.

REFERENCES

Adamson, A. W. and Gast, A. P., Wiley Interscience, New York, (1997).

Benito, P., Herrero, M., Labajos, F. M., Rives, V., Royo, C., Latorre, N. and Monzon, A., Production of carbon nanotubes from methane: Use of CO-Zn-Al catalysts prepared by microwave-assisted synthesis, *Chem. Eng. J.*, 149(1-3), 455-462(2009). doi:10.1016/j.cej.2009.02.022

Dabrowski, A., Adsorption-from theory to practice, *Adv. Colloid Interface Sci.*, 93(1-3), 135–224(2001).

Das, R., Hamid, S. B. A., Ali, M. E., Ismail, A. F., Annuar, M. S. M. and Ramakrishna, S., Multifunctional carbon nanotubes in water treatment: The present, past and future, *Desal.* 354, 160–179(2014). doi.10.1016/j.desal.2014.09.032

Dikio, E. D. and Bixa, N., Carbon nanotubes synthesis by catalytic decomposition of ethyne using Fe/Ni catalyst on aluminium oxide support, *Int. J. Appl. Chem.*, 7(1), 35-42(2011).

Dikio, E. D., Thema, F. T., Dikio, C. W. and Mtunzi, F. M., Synthesis of carbon nanotubes by catalytic decomposition of ethyne using Co-Zn-Al catalyst, *Int. J. Nanotech. Appl.*, 4(2), 117(2010).

Dubinin, M. M. and Radushkevich, L. V., Equation of the characteristic curve of activated charcoal, *Chem. Zentr.*, 1, 875–890(1947).

Farhat, S. and Scott, S. D., Review of the arc process modeling for fullerence and nanotubes production, *J. Nanosci. Nanotechnol*., 6 (5), 1189–1210(2006). doi:10.1166/jnn.2006.331

Freundlich, H. M. F., Over the adsorption in solution, *J. Phy. Chem*., 57, 385–470(1906).

Ghaedi, A. M., Ghaedi, M., Vafaei, A., Iravani, N., Keshavarz, M., Rad, M., Tyagi, I., Agarwal, S. and Gupta, V. K., Adsorption of copper(II) using modified activated carbon prepared from pomegranate wood; Optimization by bee algorithm and response surface methodology, *J. Mol. Liq*., 206, 195–206(2015). doi:10.1016/j.molliq.2015.02.029

Gong, J. L., Wang, B., Zeng, G. M., Yang, C. P., Niu, C. G., Niu, Q. Y. and Liang, Y., Removal of cationic dyes from aqueous solution using magnetic multi-wall carbon nanotubes nanocomposite as adsorbent, *J. Hazard. Mater*., 164(2-3), 1517–1522(2009). doi: 10.1016/j.jhazmat.2008.09.072

Gunay, A., Arslankaya, E. and Tosun, I., Lead removal from aqueous solution by natural and pretreated clinoptilolite: Adsorption equilibrium and kinetics, *J. Hazard. Mater*., 146(1-2), 362–371(2007).

Gupta, V. K. and Saleh, T. A., Sorptionof pollutants by porous carbon, carbon nanotubes and fullerene – An overview, *Environ. Sci. Pollut. Res*., 20(5), 2828–2843(2013a). doi: 10.1007/s11356-013-1524-1

Gupta, V. K., Agarwal, S. and Saleh, T. A., Synthesis and characterization of alumina-coated carbon nanotubes and their application for lead removal, *J. Hazard. Mater*., 185, 17–23(2011). doi: 10.1016/j.jhazmat.2010.08.053

Gupta, V. K., Kumar,R., Nayak, A, Saleh, T. A. and Barakat, M. A., Adsorptive removal of dyes from aqueous solution onto carbon nanotubes: A review, Adv. Colloid Interf. Sci. 193-194, 24–34(2013b). doi: 10.1016/j.cis.2013.03.003

Gupta, V. K., Sadegh, H., Yari, M., Shahryari-Ghoshekandi, R., Maazinejad, B. and Chahardori, M., Removal of ammonium ions from wastewater: A short review in development of efficient methods, *Glob. J. Environ. Sci. Manag*., 1(2), 149–158(2015). doi: 10.7508/GJESM.2015.02.007

Gupta, V. K., Tyagi, I., Agarwal, S., Sadegh, H., Shahryari-Ghoshekandi, R., Yari, M. and Yousefi-Nejat, O., Experimental study of surfaces of hydrogel polymers HEMA, HEMA-EEMA-MA and PVA as adsorbent for removal of azo dyes from liquid phase, *J. Mol. Liq*., 206, 129–136(2015).

Iijima, S. and Ichihashi, T., Single-shell carbon nanotubes of 1-nm diameter, *Nature*, 363, 603–605(1993). doi:10.1038/363603a0

Iijima, S., Helical microtubules of graphitic carbon, Nature, 354 (6348) 56–58(1991). doi:10.1038/354056a0

Jin, W. J., Jeon, H. J., Kim, J. H., Youk, J. H., A study on the preparation of poly(vinyl alcohol) nanofibers containing silver nanoparticles, *Synth. Met.* 157(10-12), 454 – 459(2007). doi:10.1016/j.synthmet.2007.05.011

Khan, A. R., Ataullah, R. and Al-Haddad, A., Equilibrium adsorption studies of some aromatic pollutants from dilute aqueous solutions on activated carbon at different temperatures, *J. Colloid Interface Sci.*, 194(1), 154–165(1997). doi:10.1006/jcis.1997.5041

Kirupha, S. D., Kalaivani, S., Vidhyadevi, T., Premkumar, M. P., Baskaralingam, P., Sivanesan, S. and Ravikumar, L., Effective removal of heavy metal ions from aqueous solutions using a new chelating resin poly[2,5-(1,3,4-thiadiazole)-benzalimine]: Kinetic and thermodynamic study, *J. Wat. Reuse Desal*., 6(2), 310-324(2015). doi:10.2166/wrd.2015.013).

Langmuir, I., The adsorption of gases on plane surfaces of glass, mica and platinum, *J. Am. Chem. Soc*., 40(9), 1361–1403(1918). doi:10.1021/ja02242a004

Liang, Z., Wang, Y. X., Zhou, Y. and Liu, H., Coagulation removal of melanoidins from biologically treated molasses wastewater using ferric chloride, *Chem. Eng. J*., 152(1), 88–94(2009). doi:10.1016/j.cej.2009.03.036

Liu, J., Shao, M., Li, Q., Wu, J., Xie, B., Zhang, S. and Qian, Y., Benzene-thermal route to carbon nanotubes at a moderate temperature, *Carbon*, 40, **2961-2973**(2000).

Mahmoodian, H., Moradi, O., Shariatzadeha, B., Saleh, T. A., Tyagi, I., Maity, A., Asif, M. and Gupta, V. K., Enhanced removal of methyl orange from aqueous solutions by poly HEMA-Chitosan-MWCNT nano-composite, *J. Mol. Liq*., 202, 189–198(2014). doi:10.1016/j.molliq.2014.10.040

Marti, N., Bouzas, A., Seco, A. and Ferrer, J., Struvite precipitation assessment in anaerobic digestion processes, *Chem. Eng. J*., 141 (1), 67–74(2008). doi:10.1016/j.cej.2007.10.023

Murugesan, A., Vidhyadevi, T., Kalaivani, S. S., Premkumar, M. P., Ravikumar, L. and Sivanesan, S., Kinetic and thermodynamic studies on the removal of Zn2+ and Ni 2i+ from their aqueous solution using poly(pheylthiourea)imine, *Chem. Eng. J*. 197, 368-378(2012). doi:10.1016/j.cej.2012.05.027

Nekouei, F., Nekouei, S., Tyagi, I. and Gupta, V. K., Kinetic, thermodynamic and isotherm studies for acid blue 129 removal from liquids using copper oxide nanoparticle-modified activated carbon as a novel adsorbent, J. Mol. Liq. 201, 124–133(2015). doi:10.1016/j.molliq.2014.09.027

Nyamori, V. O., Mhlanga, S. D. and Coville, N. J., The use of organometallic transition metal complexes in the synthesis of shaped carbon nanomaterials, J. Organomet. Chem., 693(13), 2205-2222(2008). doi:10.1016/j.jorganchem.2008.04.003

Rafique, M. M. A. and Iqbal, J., Production of caron nanotubes by different routes-A review, *J. Encapsulation Adsorpt. Sci*., 1 (2), **29-34**(2011). doi:10.4236/jeas.2011.12004

Redlich, O. and Peterson, D. L., A useful Adsorption isotherm, *J. Phys. Chem*., 63(6), 1024-1026(1959). doi:10.1021/j150576a611

Roberts, J. D. and Caserio, M. C., Basic Principles of Organic Chemistry, 2nd ed. W.A. Benjamin Incorporation, London, 1977.

Sadegh, H., Shahryari-Ghoshekandi, R., Agarwal, S., Tyagi, I., Asif, M. and Gupta, V. K., Microwave-assisted removal of malachite green by carboxylate functionalized multi-walled carbon nanotubes: Kinetics and equilibrium study, *J. Mol. Liq*., 206, 151–158(2015b). doi:10.1016/j.molliq.2015.02.007

Sadegh, H., Shahryari-Ghoshekandi, R., Tyagi, I., Agarwal, S. and Gupta, V. K., Kinetic and thermodynamic studies for alizarin removal from liquid phase using poly-2-hydroxyethyl methacrylate (PHEMA), *J. Mol. Liq*., 207, 21–27(2015a). doi:10.1016/j.molliq.2015.03.014

Shahryari-Ghoshekandi, R. and Sadegh, H., Kinetic study of the adsorption of synthetic dyes on graphene surfaces, *Jordan J. Chem*., 9 (4), 267–278(2014).

Shooto, D. N. and Dikio, E. D., Morphological characterization of Soot from the combustion of candle wax, *Int. J. Electrochem. Sci*., 6, 1269 – 1276(2011).

Temkin, M. J. and Pyzhev, V., Recent modifications to Langmuir isotherms, *Acta Physicochim. URSS*, 12, 217–225(1940).

Sips, R., On the structure of a catalyst surface, *J. Chem. Phys.*, 16, 490–495(1948). doi:10.1063/1.1746922

Terrones, M., Science and Technology of the twenty-first century: Synthesis, properties and applications of carbon nanotubes, *Annu. Rev. Mater. Res*., 33 (1) 419–501(2003). doi:10.1146/annurev.matsci.33.012802.100255

Toth, J., State equations of the solid gas interface layer, *Acta Chim. Acad. Sci. Hung*., 69, 311-317(1971).

Vidhyadevi, T., Murugesan, A., Kirupha, A. D., Baskaralingam, P., Ravikumar, L. and Sivanesan, S., Adsorption of Congo Red dye over pendent chlorobenzylidine rings present on polythioamide resin : Kinetic and equilibrium studies, *Separ. Sci. Technol.*, 48(10), 1450-1458(2013). doi:10.1080/01496395.2012.726306

Vijayaraghavan, K., Padmesh, T. V., Palanivelu, K. and Velan, M., Biosorption of nickel(II) ions onto sargassum wightii: Application of two-parameter and three-parameter isotherm models, *J. Hazard. Mater. B*., 133(1-3), 304 –308(2006). doi:10.1016/j.jhazmat.2005.10.016

Wang, X., Lu, J. and Xing, B. S., Sorption of organic contaminants by carbon nanotubes : Influence of adsorbed organic matter, *Environ. Sci. Technol*. 42 (9), 3207–3212(2008). doi: 10.1021/es702971g

Zare, K., Sadegh, H., Shahryari-Ghoshekandi, R., Maazinejad, B., Ali, V., Tyagi, I., Agarwal, S. and Gupta, V. K., *J. Mol. Liq.*, 212, 266-271(2015).